Slow- and fast-twitch rat hind limb skeletal muscle phenotypes 8 months after spinal cord transection and olfactory ensheathing glia transplantation

Pilar Negredo[1], José-Luis L. Rivero[2], Beatriz González[1], Almudena Ramón-Cueto[3] and Rafael Manso[1]

[1]*Centre of Molecular Biology 'Severo Ochoa' (CSIC-UAM), Autonomous University of Madrid, E-28049 Cantoblanco, Madrid, Spain*
[2]*Laboratory of Muscular Biopathology, Department of Comparative Anatomy and Pathological Anatomy, Faculty of Veterinary Science, University of Cordoba, E-14014 Cordoba, Spain*
[3]*Neural Regeneration Laboratory, Institute of Biomedicine (CSIC), E-46010 Valencia, Spain*

Paralysed skeletal muscle of rats with spinal cord injury (SCI) undergoes atrophy and a switch in gene expression pattern which leads to faster, more fatigable phenotypes. Olfactory ensheathing glia (OEG) transplants have been reported to promote axonal regeneration and to restore sensory-motor function in animals with SCI. We hypothesized that OEG transplants could attenuate skeletal muscle phenotypic deterioration and that this effect could underlie the functional recovery observed in behavioural tests. A variety of morphological, metabolic and molecular markers were assessed in soleus (SOL) and extensor digitorum longus (EDL) muscles of spinal cord transected (SCT), OEG-transplanted rats 8 months after the intervention and compared with non-transplanted SCT rats and sham-operated (without SCT) controls (C). A multivariate analysis encompassing all the parameters indicated that OEG-transplanted rats displayed skeletal muscle phenotypes intermediate between non-transplanted and sham-operated controls, but different from both. A high correlation was observed between behaviourally tested sensory-motor functional capacity and expression level of slow- and fast-twitch hind limb skeletal muscle phenotypic markers, particularly the histochemical glycerol-3-phosphate dehydrogenase activity (-0.843, $P < 0.0001$) and the fraction of variant 2s of the slow regulatory myosin light chain isoform (0.848, $P < 0.0001$) in SOL. Despite the mean overall effect of OEG transplants in patterning skeletal muscle protein expression towards normal, in 6 out of 9 animals they appeared insufficient to overcome fibre type switching and to support a consistent and generalized long-term maintenance of normal skeletal muscle characteristics. The interplay of OEG and exercise-mediated neurotrophic actions is a plausible mechanism underlying OEG transplantation effects on paralysed skeletal muscle.

(Resubmitted 3 December 2007; accepted after revision 27 March 2008; first published online 27 March 2008)

Corresponding author R. Manso: Departamento de Biología Molecular, Facultad de Ciencias, Universidad Autónoma de Madrid, E-28049 Cantoblanco, España. Email: rafael.manso@uam.es

Complete spinal cord injury (SCI) disrupts long spinal pathways and disconnects target organs from the brain. Due to failure of neurons to regenerate their axons spontaneously in the mature CNS milieu, SCI has disabling, permanent effects that include loss of voluntary movement, appearance of involuntary muscle spasms and loss of somatosensory function below the injury site. Paralysed skeletal muscle experiences progressive atrophy with reduced fibre cross-sectional area, concurrent with alterations in contractile and metabolic properties resulting from a switch in gene expression programs, particularly those governing the isoforms of the myosin subunits (see Schiaffino & Reggiani, 1996; Pette & Staron, 1997; Talmadge, 2000; Pette & Staron, 2001 for review). In

rodents with a complete spinal cord transection (SCT), the slow-twitch SOL muscle experiences a dramatic reduction in the proportion of the slow myosin heavy chain (MHC) isoform (MHC-I or β/slow), the major isoform of this muscle accounting for about 90% of the MHC content. The reduced proportion of MHC-I is compensated by increases in the fast MHC isoforms IIa and IIx/d and, to a limited extent, also IIb (Talmadge *et al.* 1995, 1999). These transitions in the MHC expression pattern are accompanied by increases in the maximal speed of shortening, in agreement with the established correlation between the MHC isoform expressed in a fibre and its maximal velocity of contraction (Reiser *et al.* 1985; Sweeney *et al.* 1986; Bottinelli *et al.* 1991). A shift

of intermediary metabolism towards more glycolytic phenotypes has also been noticed (Talmadge, 2000; Otis *et al.* 2004). Soleus muscle of SCT rats has been shown to contain a relatively high proportion of hybrid fibres co-expressing two or more different MHC isoforms (Talmadge *et al.* 1999). The persistence of hybrid fibres is taken as an indication that it represents a stable phenotypic characteristic of paralysed skeletal muscle (Talmadge, 2000). Myosin light chains (MLCs) have been reported to modulate the contractile velocity of fibres within a specified range for each MHC isoform (Bottinelli *et al.* 1994). The isoform transitions of essential (eMLCs) and regulatory (rMLCs) MLCs observed in rat skeletal muscle following SCI (Lee & Braun, 1990) could also contribute to adapt skeletal muscle contractile properties to reduced neuromuscular activity, leading to faster, more fatigable phenotypes.

Several studies have shown that interventions increasing the neuromuscular activity either by increasing the level of electrical activation or the load bearing, or both, result in transitions of MHC expression in the fast-to-slow direction, i.e. opposing the effect of SCI. These transitions follow an ordered sequence (MHC-IIb > MHC-IIx/d > MHC-IIa > MHC-I) that characterizes phenotypic changes in skeletal muscle as proposed by the theory of the continuum of MHC isoform expression (Staron & Pette, 1993). Low-frequency electrical stimulation, functional overload and resistance or endurance exercise training, among other interventions, have been shown to direct the expression of MHCs toward slower isoforms (Talmadge, 2000; Baldwin & Haddad, 2001). In addition to interventions that increase neuromuscular activity, a switch of MHC isoform expression in the fast-to-slow direction has also been observed in rat SOL and EDL muscles under conditions of hypothyroidism, glucocorticoid treatment, diabetes and ageing (see Pette & Staron, 1997 for a review).

Presently, no known treatment is capable of promoting functional regeneration across a complete spinal cord transection in humans. Paraplegic patients rely upon temporal activation of target organs by means of electrical stimulation for motor rehabilitation and improvement of bladder and bowel function (Prochazka & Mushahwar, 2001). Passive exercise and arm cranking have also been used as a palliative treatment to evoke motor automatism and to stimulate stepping (Wernig *et al.* 1999; Kjaer, 2000). These palliative strategies are consistent with experimental observations indicating that exercise or muscle activity induced by electrical stimulation can attenuate or reverse changes in skeletal muscle properties induced by SCI (Dupont-Versteegden *et al.* 1998; Hartkopp *et al.* 2003; Shields & Dudley-Javoroski, 2006).

Increasing the neuromuscular activity, as would occur upon re-establishment of functional descending upper motor neuron pathways in SCI individuals, would enable skeletal muscle protein expression pattern paralysed muscles towards normal. Among the experimental approaches developed in recent years to promote an effective regeneration of the injured spinal cord, transplantation of olfactory ensheathing glia (OEG) has evolved as one of the most promising strategies (Ramon-Cueto & Valverde, 1995; Raisman, 2001; Keyvan-Fouladi *et al.* 2002; Wewetzer *et al.* 2002; Santos-Benito & Ramon-Cueto, 2003; Barnett & Riddell, 2004). Based on histological data and behavioural tests, OEG transplantation has been reported to support axonal regeneration in the rat SC and recovery of sensory-motor function (Ramon-Cueto *et al.* 2000). In this context, we asked whether OEG transplantation could attenuate the effect of SCT on slow- and fast-twitch rat hind limb skeletal muscle phenotypes, thus contributing to preserve normal contractile properties and to favour functional recovery. Accordingly, the present investigation was aimed primarily at determining the impact of OEG transplants on the phenotypic features of fast- and slow-twitch hind limb skeletal muscles of rats with completely transected spinal cords. A second aim of this research was to test whether motor functional capacity of OEG-transplanted rats, previously determined by means of behavioural tests for the same animals of this study (Ramon-Cueto *et al.* 2000), correlated with the extent that affected slow (SOL) and fast-twitch (EDL) skeletal muscle approached normal phenotype. Finally, this investigation was also aimed at defining sensitive markers of skeletal muscle phenotype potentially valuable to assess on a quantitative basis changes in the locomotor capacity of SCT animals in response to OEG transplantation.

Methods

Preparation of adult olfactory bulb OEG for transplantation into damaged spinal cord

Preparation of adult rat olfactory bulb OEG was performed following a previously described procedure (Ramon-Cueto & Nieto-Sampedro, 1992). Olfactory bulbs were dissected from adult Wistar Hannover rats (2–2.5 months old, Charles River), killed by decapitation under deep ketamine anaesthesia (Imalgene, Rhone Merieux, Lyon; 15 mg (100 g body weight)$^{-1}$, i.p.). The olfactory bulbs of one rat per transplanted animal were dissected from the heads under sterile conditions. The first two olfactory bulb layers were dissected in Hank's balanced salt solution with calcium and magnesium ions (HBSS, Gibco) and incubated for 10 min at 37°C with 0.25% trypsin (w/v, Sigma) in a sterile tube containing 5 ml of HBSS–EDTA (without calcium and magnesium, 1 mM EDTA). Treatment with trypsin was stopped by adding D/F-10S (DEMEM and Ham's F-12 media, 1 : 1, Gibco, supplemented with 10% fetal bovine serum, 100 U ml^{-1}

penicillin and 100 μg ml^{-1} streptomycin). After washing several times with D/F-10S and centrifuging, cells were dissociated in 1 ml D/F-10S using a fire-polished Pasteur pipette. Cells from two olfactory bulbs were seeded onto one poly L-lysine (10 000–30 000 MW, Sigma)-coated culture flask (25 cm^2, Falcon) and cultured in D/F-10S at 37°C and 5% CO_2. Culture medium was changed every 2–3 days.

Seven days after plating, cells were detached from the flasks using 0.1% trypsin (w/v) in Ca^{2+}–Mg^{2+}-free HBSS medium. P75 receptor-expressing OEG were purified by immunoaffinity using an antibody against p75 (hybridoma 192, kindly provided by Dr Patrick Wood, Miami Project to Cure Paralysis), as previously described (Ramon-Cueto *et al.* 1998, 2000). Briefly, 96 mm Petri dishes were treated with biotinylated anti-mouse IgG (1/1000; Jackson Immunoresearch) for 12 h at 4°C, and thereafter with the supernatant of hybridoma 192 (1/5) containing mouse anti-p75, also for 12 h at 4°C, and washed with DMEM. Cells detached from culture flasks were seeded onto treated Petri dishes (at a ratio of two flasks per Petri dish). Unbound cells were discarded. Bound cells were detached from the dishes with a cell scraper and seeded onto poly L-lysine-treated 25 cm^2 flasks (two dishes per flask). P75-OEG were cultured in D/F-10S for no more than 2 weeks to avoid senescence. Two days after plating 2 μM forskolin (Sigma) and 20 μg ml^{-1} bovine pituitary extract (Biomedical Technologies Inc.) were added to the culture medium, and these components maintained during the whole culture period. Medium was changed every 2–3 days. For transplantation we used only p75 immunoreactive OEG, the only OEG capable of axon enfolding (Ramon-Cueto *et al.* 1993). Just before transplantation, cells were detached from the flasks, labelled with bisbenzimide (Hoechst 33342; Sigma) and re-suspended in DMEM at a density of 10^5 cells μl^{-1}.

Spinal cord transection and OEG transplantation, animal care and post-surgery period

For the experiments described in this paper we used SOL and EDL muscles of the same rats that served as experimental animals in a previous study (Ramon-Cueto *et al.* 2000). The experimental details concerning tissue culture, surgical procedures, analysis of recovery of motor and sensory functions and spinal cord histology, have been described in detail therein. Briefly, OEG were obtained from olfactory bulbs of adult Wistar rats (2.5 months old, from the animal facilities of the Centre for Molecular Biology, CSIC-Autonomous University of Madrid), expanded in culture and p75-positive cells (p75OEG) purified as reported previously (Ramon-Cueto & Nieto-Sampedro, 1992, 1994). Three weeks after plating the primary cultures (2 weeks after OEG purification) p75OEG cells were detached from the flasks, labelled

with a nuclear fluorochrome, re-suspended in culture medium and used for transplantation. Twenty-eight adult female Wistar rats (2.5 months old, 200–230 g) were anaesthetized using a mixture, in the same syringe, of 0.04 ml of medetomidine (Domtor, Pfizer) and 0.15 ml of ketamine (from a stock of 25 mg ml^{-1}). The need for supplemental doses of anaesthesia was assessed by evaluating the withdrawal reflex in both the fore and hind paws, after pin prick/dull stimulation of the wrist and ankle joints, respectively, and the tail. A laminectomy was performed in all animals to expose thoracic segments 8 and 9 (T8–T9). In 19 rats the dura was opened and the spinal cords exposed and sectioned with microscissors. The stumps were lifted to ensure completeness of the lesion. Nine paraplegic rats (SCT + CT animals, $n = 9$) received stereotaxic injections of Hoechst-labelled OEG in both cord stumps, into four sites, at the middle line, and at 1 mm from the stump border, using a sterile glass needle as previously described (Ramon-Cueto *et al.* 1998, 2000). Each site received 0.5 μl of a suspension containing 50 000 cells (200 000 per stump). Spinal cord transected, non-transplanted animals (SCT, $n = 11$) were injected with 0.5 μl of medium devoid of cells in the same spinal cord locations. Eight rats were sham operated (C, control un-injured group, $n = 8$); no spinal cord transection and no injections were performed. The injury site was covered with gelfoam, the muscles and skin were sutured and then washed with antiseptic solution. Animals were kept on a heating pad until they were completely awake. Right after surgery, all rats received a subcutaneous injection of 1 ml of lactate Ringer solution and magnesium metamizol (Nolotil, Boeringer Ingelheim) as analgesic. Augmentine (amoxyciline–clavulanic acid, 1 g–200 mg, GlaxoSmithKline), was administered at that time and twice more every 8 h. Bladder expression was performed twice a day until establishment of reflex voidance (approximately 10 days). After this period, residual urine was emptied every day from the bladder of all paraplegic rats to diminish the risk of infections. Any complication derived from the spinal cord lesion (i.e. bladder infection, autonomic disreflexia, ulcers, failure of the kidneys, among others) that occurred during the post-surgery period, was treated following protocols adapted from those used in human patients at the Spinal Cord Injury Unit of the University Hospital La Fe, Valencia, and the National Paraplegics Hospital of Toledo, Spain (see Santos-Benito *et al.* (2006) for a detailed description of the post-operative care of these paraplegic rats). After recovery from surgery, all animals were left to move (or try moving) freely in an open field every day for 20 min and were trained to climb onto inclined grids of different level of difficulty as a function of the slope. From 3 to 7 months post-surgery the improvement of motor and sensory function was analysed in all rats (Ramon-Cueto *et al.* 2000). Recovery of voluntary movement of the hind limbs was assessed

Table 1. Characteristics of anti-myosin heavy chain (MHC) monoclonal antibodies (MAb) and clues for the immunohistochemical identification of the MHC isoforms expressed in skeletal muscle fibres

	MAb designation[1]				
	BF-F8	SC-71	BF-35	RT-D9	BF-F3
Class	IgG	IgG	IgG	IgM	IgM
Working dilution	1 : 200	1 : 10 000	1 : 10 000	1 : 1000	1 : 25
Specificity[2]			All except	MHC-IID/X	
	MHC-I	MHC-IIA	MHC-IID/X	and MHC-IIB	MHC-IIB
MHC content	MAb reactivity				
I	+	−	+	−	−
I + IIA	+	+	+	−	−
IIA	−	+	+	−	−
IIAD/X	−	+	+	+	−
IID/X	−	−	−	+	−
IID/XB	−	−	+	+	+
IIB	−	−	+	+	+

[1]Source: S. Schiaffino, Padova, Italy. [2]According to Schiaffino *et al.* (1989). +, positive reaction for a MAb with a specific MHC-based fibre type. −, no reaction for a MAb and a specific MHC-based fibre type.

using a climbing test that allowed discerning between local reflex activity and real voluntary movement. Seven months post-surgery, animals received a restricted amount of standard laboratory chow (calculated on an individual basis) to maintain body weight steady in a range of 270–300 g. After this period animals were allowed to eat *ad libitum* until killing.

All animals underwent a second surgery for tracer injection 7 months and 1 week after the first surgery. They were anaesthetized with an isoflurane-based gaseous anaesthesia (induction: $2 \, l \, min^{-1} \, O_2$, $1 \, l \, min^{-1} \, N_2O$ and 3.5% isoflurane for 2 min; maintenance: $0.8 \, l \, min^{-1} \, O_2$, $0.4 \, l \, min^{-1} \, N_2O$ and 2.5% isoflurane) and received the same treatments (antibiotics and analgesics) described above. Three weeks later (8 months after the first surgery) animals were deeply anaesthetized with a mixture of Domtor and ketamine as described above, and soleus (SOL) and extensor digitorum longus (EDL) muscles of both hind limbs were dissected quickly. Immediately thereafter, all rats were perfused with saline and fixative (4% paraformaldehyde) and their spinal cords dissected for histological analysis, as previously reported (Ramon-Cueto *et al.* 2000). All experimental procedures followed the guidelines laid down by the Autonomous University of Madrid and the Higher Council of Scientific Research of Spain following the normal procedures directing animal welfare (Real Decreto 223/88, BOE of 18 of March) and adhered to the recommendations included in the Guide for Care and Use of Laboratory Animals (US Department of Health and Human Services, NIH) and European laws and regulations on the protection of animals, under the advice of specialized personnel.

Muscle dissection and preparation of tissue samples

Eight months after the first intervention, all animals were weighed and anaesthetized as indicated earlier in this section. SOL and EDL muscles of both hind limbs were dissected quickly. Individual muscles were weighed. Tissue blocks were prepared from the muscle belly in isopentane chilled with liquid nitrogen and stored at $-70°C$ until analysed. Cryostat serial cross-sections prepared at $-20°C$ were placed on either gelatin-coated or silanized slides, for immunohistochemistry, or cover slips, for qualitative and quantitative histochemistry. The remainder of the muscle was frozen in liquid nitrogen and maintained at $-70°C$ until used for electrophoresis.

Immunohistochemistry and histochemistry

Immunohistochemical analysis of myosin heavy chain (MHC) isoform expression in individual fibres was performed on 10 μm thick serial cryostat cross-sections reacted with a series of monoclonal antibodies (Mabs, Table 1) specific for rat MHC isoforms (Schiaffino *et al.* 1989) as described by Rivero *et al.* (1999). Localization of the bound primary antibodies was performed with biotin-bound secondary antibodies and avidin–biotin complex (ABC, peroxidase-based kit PK-6102, for IgG class monoclonal antibodies (MAbs), and alkaline phosphatase-based kit AK-5010, for IgM class MAbs, Vector Laboratories, Burlingame, CA, USA) using diaminobenzidine (DAB, kit SK-4100; Vector Laboratories) as the chromogen to localize peroxidase and a pre-mixed NBT/BCIP solution (B.6404, Sigma, St

Louis, MO, USA) containing levamisole (SP-500) to reveal alkaline phosphatase. Background staining was controlled in additional serial sections incubated without primary antibody. Muscle fibres were classified for MHC content according to their individual patterns of Mab reactivity, as indicated in Table 1. Seven fibre types were identified, four expressing unique MHC isoforms (designated I, IIA, IID/X and IIB) and three additional mixed fibre types co-expressing two MHCs isoforms I + IIA, IIA + IIX/D (IIAD/X) and IID/X + IIB (IID/XB). Two additional serial cross-sections were stained for qualitative assessment of myofibrillar ATPase activity, following alkaline (pH 10.45) and acid (pH 4.45) pre-incubations, using a modification (Nwoye *et al.* 1982) of the Brooke and Kaiser method (Brooke & Kaiser, 1970). According to the staining intensity after alkaline pre-incubation, pure muscle fibres were classified in type I (white), IIB (grey) and IIA and IID/X (black). Similarly, the mATPase reaction after acid pre-incubation also allowed distinction of fibre types according to staining intensity: type I (black), IIA (white) and IID/X and IIB (intermediate intensity). Nevertheless, a continuum of staining intensities was observed within fast-twitch subtypes (Delp & Duan, 1996). Five consecutive cross-sections were used for each enzyme histochemical assay (succinate dehydrogenase (SDH) and glycerol-3-phosphate dehydrogenase (GPDH)). Three of them were incubated in medium containing substrate (either succinic acid or glycerol-3-phosphate); the other two, incubated in the absence of substrate, were used to correct for non-specific staining. Mean muscle oxidative capacity was assessed by means of quantitative SDH histochemistry performed in $10\,\mu m$ thick sections following the procedure previously described by Blanco *et al.* (1988). The activity of GPDH, an indirect marker of glycolytic capacity, was determined on $14\,\mu m$ thick sections according to Martin *et al.* (1985). After staining, sections were digitized within 2–3 h with a computerized image-processing system (see below). Since SDH and GPDH activities are linear for at least 15 or 30 min, respectively, termination of the reaction within this time allowed enzymatic activities to be expressed as steady-state rates. These activities were expressed as optical density per time unit ($OD\,min^{-1}$).

Quantitative tissue analysis

After appropriate staining, a region ($750\,000\,\mu m^2$) of the cross-sections containing between 125 and 175 fibres per muscle sample was selected for further analysis. Serial sections were surveyed to find regions free of artefacts. They were visualized and analysed using a Leica DMLS microscope (Leica Microsistemas, Barcelona, Spain), a high-resolution colour charge-coupled device Leica ICCA camera (Leica Microsistemas, Barcelona, Spain), and an eight-bit Matrox Meteor II frame-grabber (Matrox

Electronic Systems Ltd, Barcelona, Spain), combined with an image-analysing software (Visiolog 5, Noemi, Microptic, Barcelona, Spain). Serial sections were systematically digitized and the fibres numbered at random and classified with their immunohistochemical stains. The fibre type distribution of each muscle sample was established following immunohistochemistry by counting the relative frequency of the various fibre types. The same region of the serial sections stained for quantitative SDH and GPDH was digitized as a grey level (range of grey level 0–255) image. For each sample analysed, a mean optical density (OD) was determined for each quantitative histochemical assay and values reported as $OD\,min^{-1}$. For each enzyme assay, the mean value of the three sections analysed with substrate minus the mean of the two tissue blank sections was used to calculate the enzyme activity of a single muscle sample. Since a number of factors can influence the reliability of histochemical enzyme activity determination, we examined the measurement precision associated with several sources of variability (thickness of the tissue, image analysis system, etc.) by repeated measurements on the same single fields in three consecutive sections. The coefficient of variation for triplicate measurement of OD in each histochemical assay was always below 5%. The cross-sectional areas of 125 individual muscle fibres per sample were systematically measured with the same computerized video display image-analysis system previously described and values were averaged according with each muscle biopsy specimen. Fibre size was calculated in the histochemical preparations of SDH since this procedure has no negative impact on muscle fibre size (Snow & Guy, 1980).

Two-dimensional electrophoresis and evaluation of the relative proportions of myosin light chain (MLC) isoforms and variants thereof

Muscle homogenization, sample preparation and two-dimensional (2D) electrophoresis of proteins were performed essentially as previously described (Hernando & Manso, 1997; Gonzalez *et al.* 2002), using a pH range of 4–6.5 in the first, isoelectric focusing dimension and 9–20% acrylamide slab gel gradients for the second dimension. The resulting 2D electrophoretograms of whole muscle proteins were stained in 0.5% Coomassie brilliant blue R to determine the relative proportions of MLC isoforms. Three variants of each, the slow (s) and fast (f) regulatory (r) MLCs (designated 2s, 2s1, 2s2 and 2f, 2f1 and 2f2, respectively, from less to more acidic) were analysed as previously reported (Gonzalez *et al.* 2002). Quantification of proteins in stained gels was performed using densitometry (Bio-Rad, GS-710, with Quantity One software v.4.2.1). Optical density

measurements were performed in the linear absorption range.

Statistical and discriminant analysis of the data

Data were expressed as means ± s.d. Differences among groups were analysed by one-way analysis of variance (ANOVA) using the statistical program SPSS 8.0. Once significance was established, pair-wise comparisons were conducted using a Bonferroni *post hoc* test, when the homogeneity of variance was accepted (Levene statistics), and a Dunnett's T3 test when the homogeneity of variance was discarded. Differences were considered statistically significant at $P < 0.05$. Correlations between variables were assessed using Pearson's or Spearman's tests (for homogeneous or non-homogeneous variances, respectively). All the data from the individual muscles of all three groups were included in a multivariate, discriminant analysis using the package Statistica for Windows. This analysis allowed grouping skeletal muscles of experimental animals according to phenotype, to compare the overall characteristics of group pairs to establish their homology

and to classify individual muscles into one group or the other. Thus, muscles of OEG-transplanted animals were compared with those of non-transplanted and control to get information on the impact of OEG transplants on the relative maintenance of normal skeletal muscle characteristics. Statistically significant differences between pair of groups ($P < 0.05$) and the degree of homology of muscles from OEG-transplanted rats with those of control or non-transplanted (Mahalanobis distances) are indicated in Fig. 5 for each group pair.

Results

Muscle mass, muscle-somatic index (MSI) and fibre cross-sectional area (CSA) of paralysed rat SOL and EDL muscles 8 months after SCT: effect of OEG transplantation

Eight months after a complete spinal cord transection (SCT), the wet weights of paralysed rat SOL and EDL muscles were reduced to 56% and 76% of the control values, respectively (Fig. 1). The MSI (wet weight referred
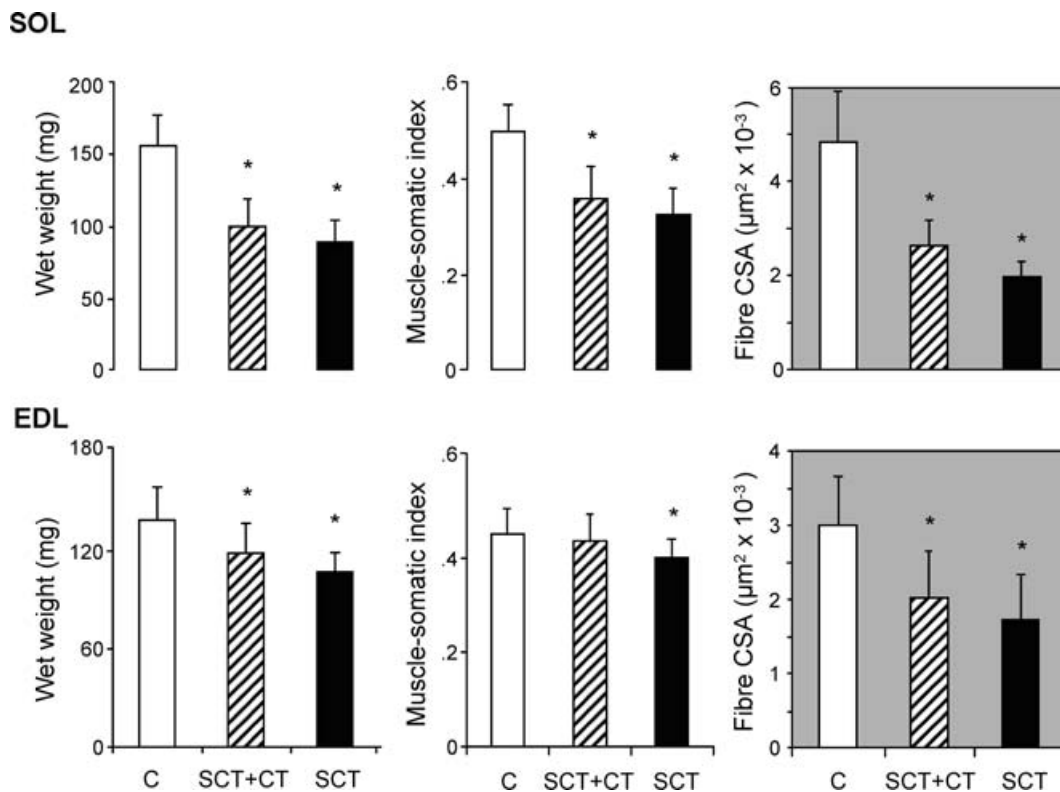
Figure 1. Morphological characteristics of fast- and slow-twitch skeletal muscles of the rat hind limb following long-term paralysis induced by a complete transversal section of the spinal cord: effect of OEG transplantation
The figure represents the absolute and relative (body weight and muscle-somatic index) wet weights and mean fibre cross-sectional area (CSA) of the slow-twitch SOL and fast-twitch EDL muscles of sham-operated controls (C, $n = 8$), spinal cord-transected (SCT, $n = 11$) and SCT, OEG-transplanted (SCT + CT, $n = 9$) rats. Data are means ± s.d. of the number of animals per group indicated above. Since both hind limbs were considered independently, the number of samples was twice the number of animals per group. *$P < 0.05$, SCT or SCT + CT *versus* sham-operated controls.

to body weight) was reduced to 66% and 82%, respectively, and the mean fibre CSA to 41% and 58%, respectively. Thus, in quantitative terms, atrophy affected the soleus muscle, mainly formed by slow-twitch fibres with a higher diameter, more than the EDL, formed essentially by fast-twitch fibres. In animals transplanted with OEG immediately after SCT, the mean wet muscle weight and fibre CSA tended to be higher than in non-transplanted animals, though differences did not reach statistical significance. Both parameters were significantly lower in transplanted animals than in sham-operated controls ($P < 0.05$). The MSI of the EDL, however, increased in OEG-transplanted animals and reached values that were not different from controls though still not different from non-transplanted SCT-animals.

Metabolic activity of paralysed rat soleus and EDL muscles 8 months after complete SCT: effect of OEG transplantation

Cordotomy had a marked effect on the metabolic properties of both skeletal muscle types, particularly of the soleus (Fig. 2). The mean histochemical glycolytic capacity of both muscle types, estimated by the indirect marker glycerol 3-phosphate dehydrogenase (GPDH), increased to 150% ($P < 0.0001$) and 117% ($P < 0.0001$) for soleus and EDL muscle, respectively. In soleus muscle, transplantation of OEG lowered the GPDH activity significantly with respect to non-transplanted animals ($P < 0.0001$) while remaining higher ($P < 0.0001$) than controls. Interestingly, in the EDL muscle of OEG-transplanted animals GPDH levels were lower than in non-transplanted animals ($P < 0.0001$) and statistically non-different from controls (Fig. 2). Thus, OEG transplantation was capable of normalizing the glycolytic activity of the EDL to control values.

The muscle oxidative capacity, measured by quantitative SDH histochemistry, tended to increase in the soleus and decrease in the EDL of cordotomized animals, when compared to controls but differences did not reach statistical significance (Fig. 2). In an apparent paradox, in the EDL muscle of OEG-transplanted animals the mean oxidative capacity was even lower than in non-transplanted animals, reaching values that were statistically different from both, control and non-transplanted animals (Fig. 2).

Expression of isoforms of the myosin heavy (MHC) and light chains (MLC) in paralysed rat soleus and EDL muscles 8 months after SCT: effect of OEG transplants

SCT induced a slow-to-fast fibre type switching in both muscle types. As the soleus is composed primarily of slow-twitch fibres its transition was more evident than that of the EDL, mainly formed by fast-twitch fibres (Fig. 3). Eight months after cordotomy, the EDL muscle showed a reduced proportion of fibres expressing the MHC isotypes I (β/slow) or IIA as compared to controls, while hybrid IID/XB fibres increased. Transplantation of OEG immediately after SCT had no significant effect on fibre type distribution in the EDL muscle, but the proportion of IID/X fibres tended to be lower. In the paralysed soleus, 8 months after SCT, the proportion of fibres expressing MHC-I was dramatically reduced while fibres expressing MHC-IIA or IID/X, either alone or in combination increased (see Fig. 3). Following OEG transplantation the proportion of type I fibres in the soleus was intermediate between non-transplanted and control animals, and statistically different from both. The proportion of type I + IIA fibres tended to be lower than in non-transplanted animals but was neither different from them nor from controls. The high standard deviation of the means (see particularly the fraction of type I fibres in the SOL of OEG-transplanted animals) is indicative of a high degree of variability in the individual responses. Although for most of the parameters tested no significant differences were observed between contralateral muscles the fibre type distribution in the EDL muscle of OEG-transplanted rats was an exception since the relative abundance of IIAD/X and IID/X fibres was higher ($P < 0.05$ and $P < 0.001$, respectively) while that of type IIB fibres was lower ($P < 0.05$) in left as compared with right hind limb muscles.

Spinal cord transection had also a marked effect on the expression of myosin light chain (MLC) isoforms. Eight months after SCT, the proportion of slow (s) isoforms of both essential (e) and regulatory (r) MLCs in paralysed SOL or EDL muscles was lower than in controls (Fig. 4a and b panels). This effect was quantitatively more prominent in the SOL (Fig. 4, upper half), where the proportion of slow isoforms of rMLCs (denoted 2s in 2D patterns of Fig. 4) was reduced to less than one fifth of control, but was also noticed in the proportion of MLC isoforms in the EDL muscle (Fig. 4, bottom half). Transplantation of OEG tended to increase the proportion of slow MLC isoforms when compared to non-transplanted animals but differences did not reach statistical significance (Fig. 4a and b panels). As previously described (Gonzalez *et al.* 2002 and depicted in Fig. 4, 2D patterns), both fast (f) and slow (s) rMLC isoforms displayed different variants with the same molecular weight and slightly different isoelectric point. In SOL, the proportion of variant 2s, the less acidic of the variants of the slow rMLC isoform and the most abundantly represented in this muscle, was greatly lowered following cordotomy. This variant was also present in EDL muscle, as a minor component of the minor (slow) isoform, and its proportion was also reduced in SCT animals in a statistically significant manner.
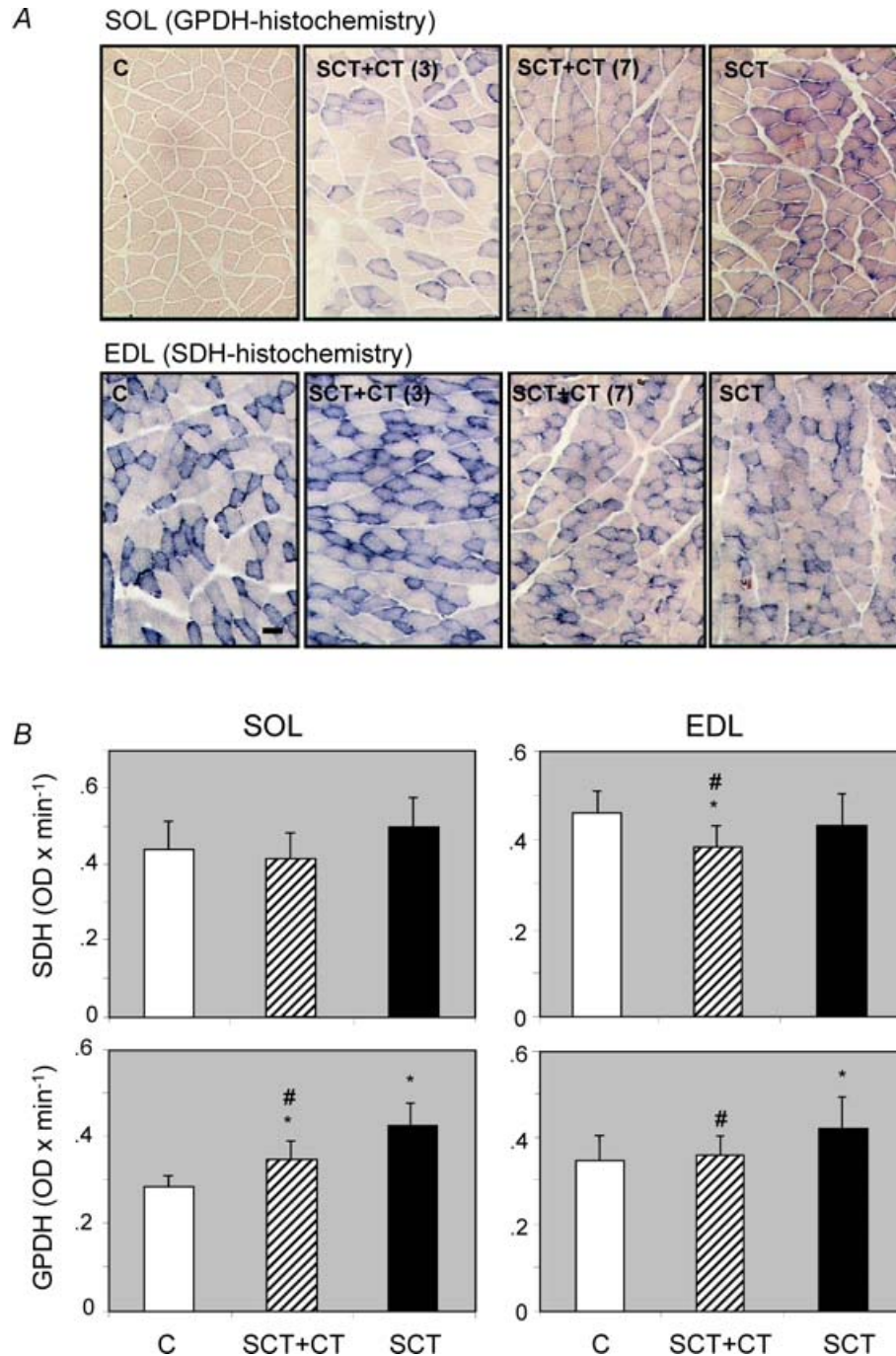
Figure 2. Histochemical changes in markers of energy metabolism in SOL and EDL muscles of the rat, induced by a complete spinal cord transection: effect of OEG transplantation

Cross-sections of soleus and EDL muscles were subjected to quantitative glycerol-3-phosphate dehydrogenase (GPDH) or succinate dehydrogenase (SDH) histochemistry, as indicated in the Methods section. *A*, representative sections of sham-operated controls (C, *n* = 8) and spinal cord-transected (SCT, *n* = 11) rats, together with two examples of SCT rats transplanted with OEGs (SCT + CT, *n* = 9) showing a different degree of functional recovery (3 and 7, good and bad recovery, respectively (Ramon-Cueto *et al.* 2000)), stained for GPDH (soleus) or SDH (EDL). *B*, graphic representation of the quantitative histochemistry data for GPDH and SDH in both muscle types. Data are means ± S.D. of the number of animals per group indicated above, corresponding to 2-fold number of samples (both hind limbs) per group. *$P < 0.05$, SCT or SCT + CT *versus* sham-operated controls. #$P < 0.05$, OEG-transpanted (SCT + CT) *versus* non-transplanted SCT-rats. Bar (situated in the control EDL muscle for SDH histochemistry) indicates 1 μm.
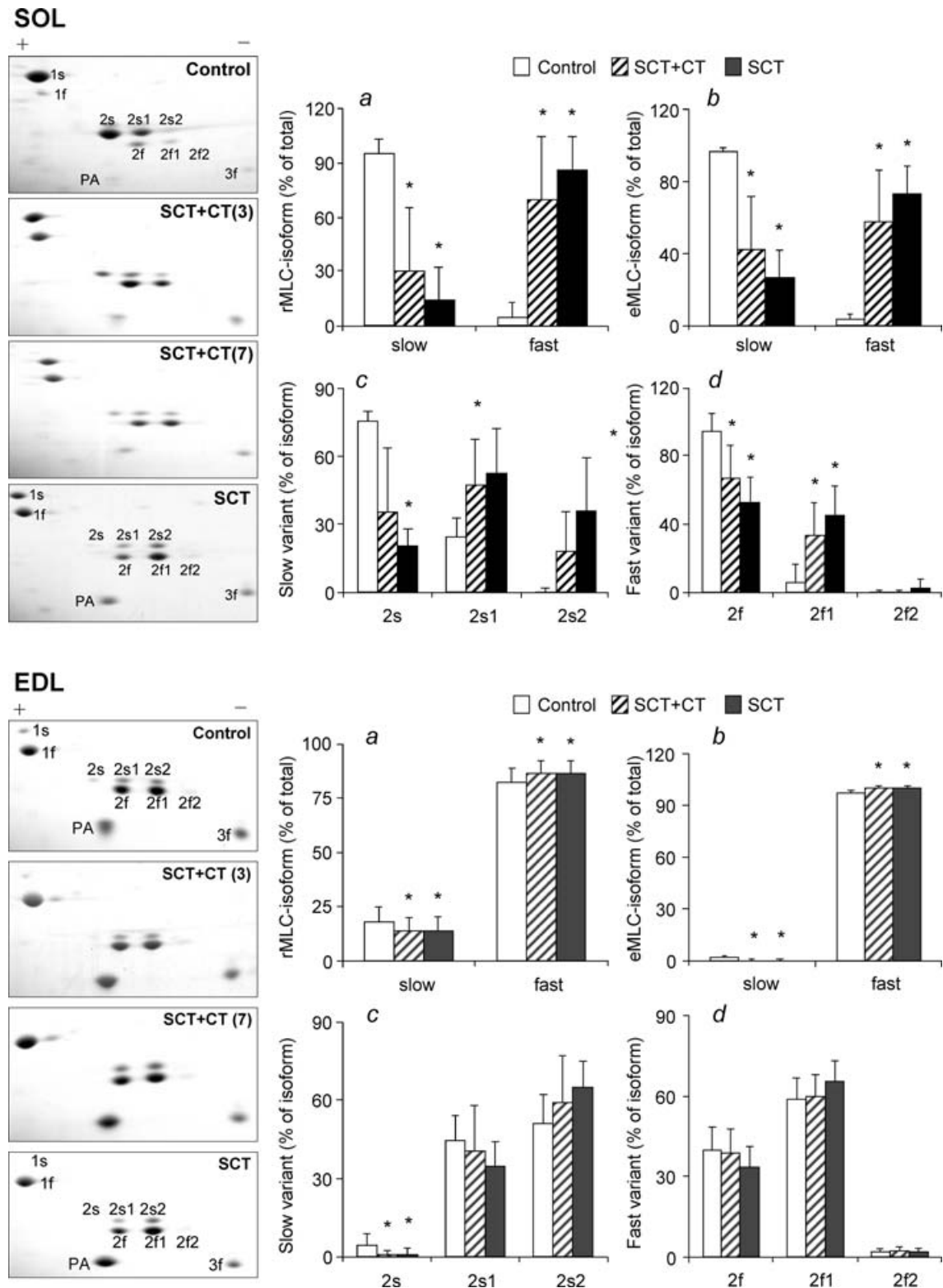
Transplantation of OEG did not restore/maintained the proportion of variant 2s in the EDL to the control level. However, in the SOL, OEG transplantation increased the proportion of this variant to a level that was statistically non-different from both control and non-transplanted animals. The high standard deviation of the data from OEG-transplanted animals further indicated a wide range of variation in the individual responses.
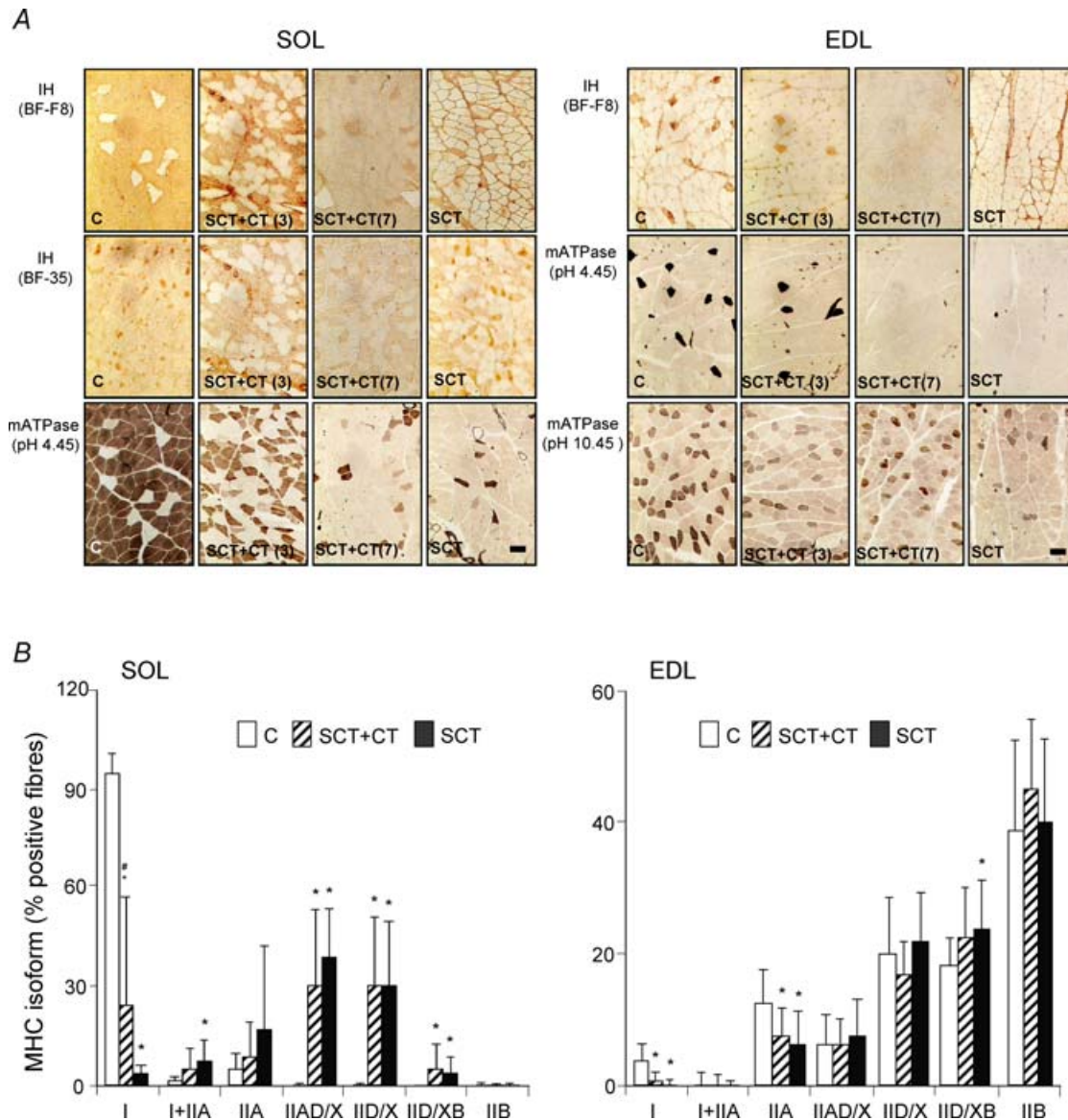
Figure 3. Fibre type transitions in soleus and EDL muscles of the rat induced by a complete transversal section of the spinal cord: effect of OEG transplantation
Fibre typing of soleus and EDL muscles was performed in serial cross-sections correlated to those shown in Fig. 2, that were probed with monoclonal antibodies directed against different myosin heavy chain (MHC) isoforms or stained for myofibrillar ATPase with pre-incubations at pH 4.45 or 10.45, as indicated in the Methods section. The antibody BF-F8 selectively recognizes MHC-I, and BF-35 all MHCs except IIX/D. Myofibrillar ATPase after acid pre-incubation at pH 4.45 denotes three staining intensities: dark (type I), intermediate (IID/X and IIB) and light (IIA). Myofibrillar ATPase after alkaline pre-incubation at pH 10.45 delineates three staining intensities corresponding to type I (light), IIA and IID/X (dark) and IIB (intermediate) fibres. *A*, representative samples of soleus and EDL muscles of sham-operated (C, $n = 8$) and SCT ($n = 11$) together with two examples of SCT rats transplanted with OEGs (SCT + CT, $n = 9$) with different level of functional recovery (3 and 7, represent good and bad recovery, respectively). *B*, graphic representation of the proportions of pure (expressing only one MHC isoform) and hybrid (expressing two MHC isoforms) fibres in both muscle types. Data are means ± S.D. of the number of animals per group indicated above corresponding to twice the number of samples (both hind limbs were considered independently). *$P < 0.05$, SCT or SCT + CT *versus* sham-operated; #$P < 0.05$, SCT + CT *versus* non-transplanted SCT rats. Bars in the SCT panels corresponding to mATPase histochemistry for SOL (pH 4.45) and EDL (pH 10.45) muscles indicate 1 μm.

Figure 4. Transitions of essential (e) and regulatory (r) myosin light chain (MLC) isoforms and variants thereof, in soleus and EDL muscles of the rat following a complete transversal section of the spinal cord: effect of OEG transplantation

The proportions of e- and rMLC isoforms and of their variants, in soleus or EDL muscles were determined in Coomassie blue-stained two-dimensional (2D) electrophoretograms of whole muscle protein homogenates, as indicated in the Methods section. Different variants of the slow (s) and fast (f) rMLC (denoted 2s, 2s1 and

Global analysis of slow- and fast-twitch skeletal muscles of cordotomized rats following OEG transplantation based on expression of phenotypic markers

To establish the degree of similarity between muscles of OEG-transplanted and those of control and non-transplanted cordotomized animals, a multivariate discriminant analysis was performed with all the data available for each muscle, including left and right hind limbs as independent values. The discriminant model for the SOL included the following variables: wet weight, muscle-somatic index, percentage of type I, I + IIA, IIA, IIAD/X and IIX fibres, SDH and GPDH activities, fibre CSA, slow rMLC/total rMLC, slow eMLC/total eMLC, variant 2s/total rMLC, variant 2s/slow rMLC, variant 2f/total rMLC and variant 2f/fast rMLC. For the EDL muscle the same parameters were considered though the fraction of type IID/XB and IIB fibres was included instead of that of type I and IIA. With these parameters, the percentages of correctly classified observations were 100, 90.9, 77.8 and 89.3 in the SOL and 100, 95.45, 94.43 and 96.42 in EDL muscle, for samples of control, non-transplanted, OEG-transplanted and whole group of animals, respectively. None of the 44 individual skeletal muscles (soleus and EDL, left and right hind limbs) from SCT, non-transplanted animals displayed characteristics of control animal muscle (and only 3 could be classified as originating from OEG-transplanted animals). In OEG-transplanted rats 31 out of 36 muscles were classified correctly, 4 as deriving from SCT and only 1 from control animals. On a per muscle type basis, contrary to expected, the percentage of correctly classified observations in the EDL was still higher than in the SOL.

The Mahalanobis distances between group pairs and their statistical significance in both muscle types are indicated in Fig. 5. The data highlight the differences between the overall phenotypic characteristics of muscles of OEG-transplanted animals and those of both control and non-transplanted. Thus, with respect to skeletal muscle phenotype, OEG-transplanted rats built a separate group, situated between control and non-transplanted, with overall properties still closer to non-transplanted animals than to controls as deduced from their relative Mahalanobis distances.

Correlation of previously published data from functional tests with the expression of morphological, metabolic and contractile activity markers in fast- and slow-twitch skeletal muscle of cordotomized rats following OEG transplantation

In general terms, practically all the phenotypic markers measured in this investigation for SOL or EDL muscles correlated very well with previously published data from functional capacity derived from behavioural tests (graded from 0 to 4 as previously described in Ramon-Cueto *et al.* 2000). In soleus muscle, wet weight, muscle-somatic index, percentage of fibres expressing only MHC-I (type I fibres), fraction of slow rMLC isoform from total rMLC (slow rMLC/total rMLC), fraction of slow eMLC isoform from total eMLC (eMLCs/total eMLCt), fraction of variant 2s from total rMLC and fraction of variant 2s from slow rMLC showed a positive, statistically significant correlation, while the fraction of type IIAD/X or IID/X fibres, SDH and GPDH activities, fraction of variant 2f from total rMLC and fraction of variant 2f from fast rMLC correlated negatively. On the basis of the amplitude of the changes induced by SCT and the degree of maintenance of normal values following OEG transplantation, four of these parameters were considered tentatively as candidate sensitive markers of paralysed soleus muscle phenotype: (1) glycolytic activity, as measured by quantitative GPDH histochemistry (Pearson's correlation, $r = -0.843$, $P < 0.0001$); (2) proportion of fibres expressing the MHC-I (β/slow) as the unique MHC isoform (Spearman's correlation, $r = 0.764$, $P < 0.0001$); (3) fraction of slow isoform from the total rMLC complement (Spearman's correlation, $r = 0.746$, $P < 0.0001$; and (4) fraction of the variant 2s from total slow rMLC isoform (Spearman's correlation, $r = 0.848$, $P < 0.0001$). Figure 6 represents the mean values of these parameters in control (C) and paralysed (SCT) right and left hind limb SOL together

---

2s2 and 2f, 2f1 and 2f2, from less to more acidic, respectively) were identified as reported previously (Gonzalez *et al.* 2002). The figure reproduces representative 2D patterns together with the graphic representation of the percentage distributions of r- and eMLC isoforms (panels *a* and *b*) and rMLC variants (panels *c* and *d*) in SOL (upper panel) and EDL (bottom panel) muscles. C, sham-operated controls (*n* = 8); SCT, spinal cord-transected (*n* = 11), SCT + CT, SCT rats transplanted with OEGs (*n* = 9). The 2D patterns of MLCs correspond to the same muscles used as representative examples in Figs 2 and 3 (SCT + CT, 3 and 7, representing two examples of rats with good and bad functional capacity as determined by behavioural tests). 1s, 1f and 3f, fast (f) and slow (s) isoforms of essential MLCs; 2s, 2s1, 2s2 and 2f, 2f1 and 2f2, charge variants of the slow (s) and fast (f) regulatory MLC isoforms, from less to more acidic. + and − in the upper part of the 2D patterns indicate the sides of basic and acidic isoelectric points, respectively. Data are means ± s.d. of the number of animals per group indicated above, corresponding to twice the number of muscles. *$P < 0.05$, SCT or SCT + CT *versus* sham-operated controls.
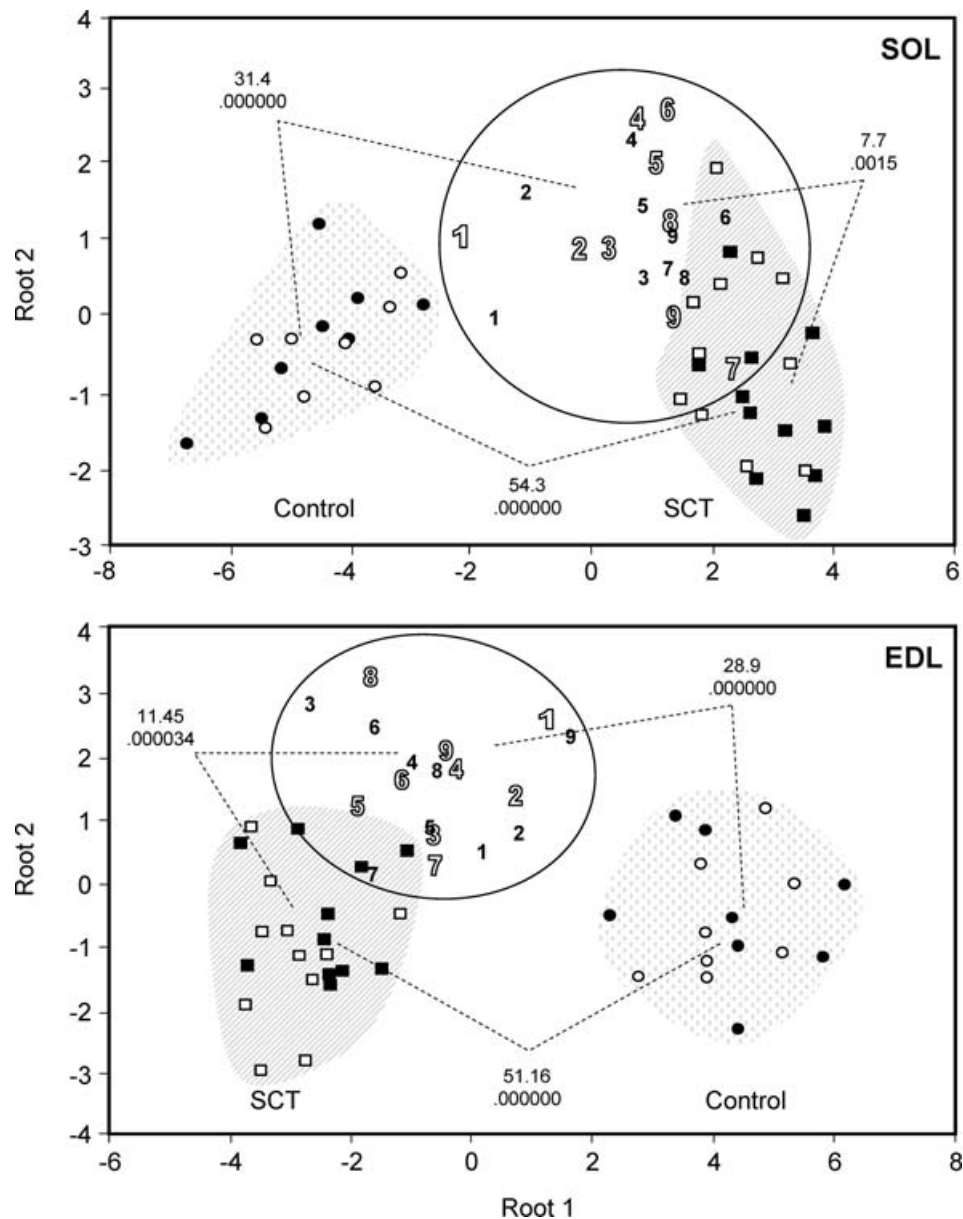
Figure 5. Phenotypic classification of individual hind limb muscles of OEG-transplanted rats in relation to non-transplanted and sham-operated controls by means of multivariate discriminant analysis
Individual SOL and EDL muscles of left and right hind limbs of all experimental rats were classified into different groups as a function of a cohort of phenotypic characteristics by means of discriminant analysis. The discriminant model for the SOL included the following variables: wet weight, muscle-somatic index, percentage of fibre types I, I + IIA, IIA, IIAD/X and IIX/D, SDH, GPDH, CSA, fraction of slow rMLC isoform from total rMLC (rMLCs/rMLCt), fraction of slow eMLC isoform from total eMLC (eMLCs/eMLCt), variant 2s/rMLCt, variant 2s/rMLCs, variant 2f/rMLCt and variant 2f/rMLCf. The same parameters were considered also for the EDL muscle, except that the percentage of fibre types IIX/DB and IIB was taken instead of types I and IIA. Circles represent the relative distribution of sham-operated rat control muscles when all the phenotypic markers mentioned above are considered together; squares represent SCT rats; 1–9 refer to individual SCT + CT animals, numbered from best (1) to worst (9) recovered according to the scores of behavioural tests (Ramon-Cueto *et al.* 2000). Open and filled symbols represent left and right hind limb muscles, respectively. For both muscle types, OEG-transplanted animals configure an independent phenotypic group, different from both control and SCT animals. The squares of the Mahalanobis distances between pairs of groups indicative of the relative phenotypic divergences are indicated together with the *P* values for the statistical significance of the comparisons between pairs of groups.

with the individual values obtained for left and right SOL in each of the OEG-transplanted animals, ordered from 1 to 9 according to previously reported time course and amplitude of recovery of sensory-motor functions (Ramon-Cueto *et al.* 2000), represented in Fig. 6*A*. It may be observed in this figure that all four parameters allowed a good discrimination between muscles from animals that recovered sensory and motor function within the first 3 months after the intervention and those that showed the first signs of recovery at the final part of the 8 month period. From the data of Fig. 6 it is derived that all four phenotypic markers identified rats 1, 2 and 3 as the animals with skeletal muscle characteristics closest to normal, in this order, and rat 9 as the farthest. The remaining five animals were ordered in slightly different positions as a

function of the parameter considered. GPDH activity and the fraction of variant 2s from the slow rMLC isoform were the only parameters that provided enough sensitivity to allow animals with similar motor functional capacity to be graded according to expression of a molecular marker. Considering a mean between both hind limb muscles, both parameters allowed OEG-transplanted animals to be ordered in the sequence 1, 2, 3, 4(6), 6(4), 8, 7, 5, 9. Similar conclusions were derived from the analysis of almost the same parameters in the EDL muscle (not shown). For this muscle, GPDH activity (Spearman's correlation $r = -0.604$, $P < 0.0001$) and wet muscle weight (Pearson's correlation $r = 0.613$, $P < 0.0001$) (or muscle-somatic index) showed the highest discriminatory potential.

Figure 6. Correlation of data from behaviourally tested functional recovery and expression of selected phenotypic markers of SOL muscle
Muscles were obtained from anaesthetized animals 1 month after the last test of functional recovery was passed, 8 months after the intervention for SCT and OEG transplantation. *A*, results from behavioural tests (contact placing, C, and proprioceptive, P, responses) performed 3, 5 and 7 months after the intervention, as reported previously (Ramon-Cueto *et al.* 2000). B, L and R refer to detection of recovery in both, left or right hind limb(s), respectively. *B*, percentage of type I fibres assessed by immunohistochemistry. *C*, proportion of slow rMLC from the whole rMLC complement, obtained from densitometry of Coomassie blue-stained 2D electrophoretograms. *D*, fraction of the less acidic isoelectric point variant (2s) from the slow rMLC isoform, obtained as in *C*. *E*, mean glycerol-3-phosphate dehydrogenase activity (GPDH) determined by quantitative histochemistry. Data for left and right hind limb muscles of control (C, sham-operated animals, $n = 8$) and SCT-rats ($n = 11$) are means ± S.D. of all animals of the group. 1–9 refer to the individual muscles of the group of rats with completely transected spinal cord that received OEG transplants, ordered from best (1) to worst (9) recovered according to previously published scores from functional tests (Ramon-Cueto *et al.* 2000). *A* is a modification of Fig. 1 from the above-mentioned reference. The correlations of these parameters with the scores of functional capacity (as assessed by means of behavioural tests) are indicated together with the statistical significance of the observation.
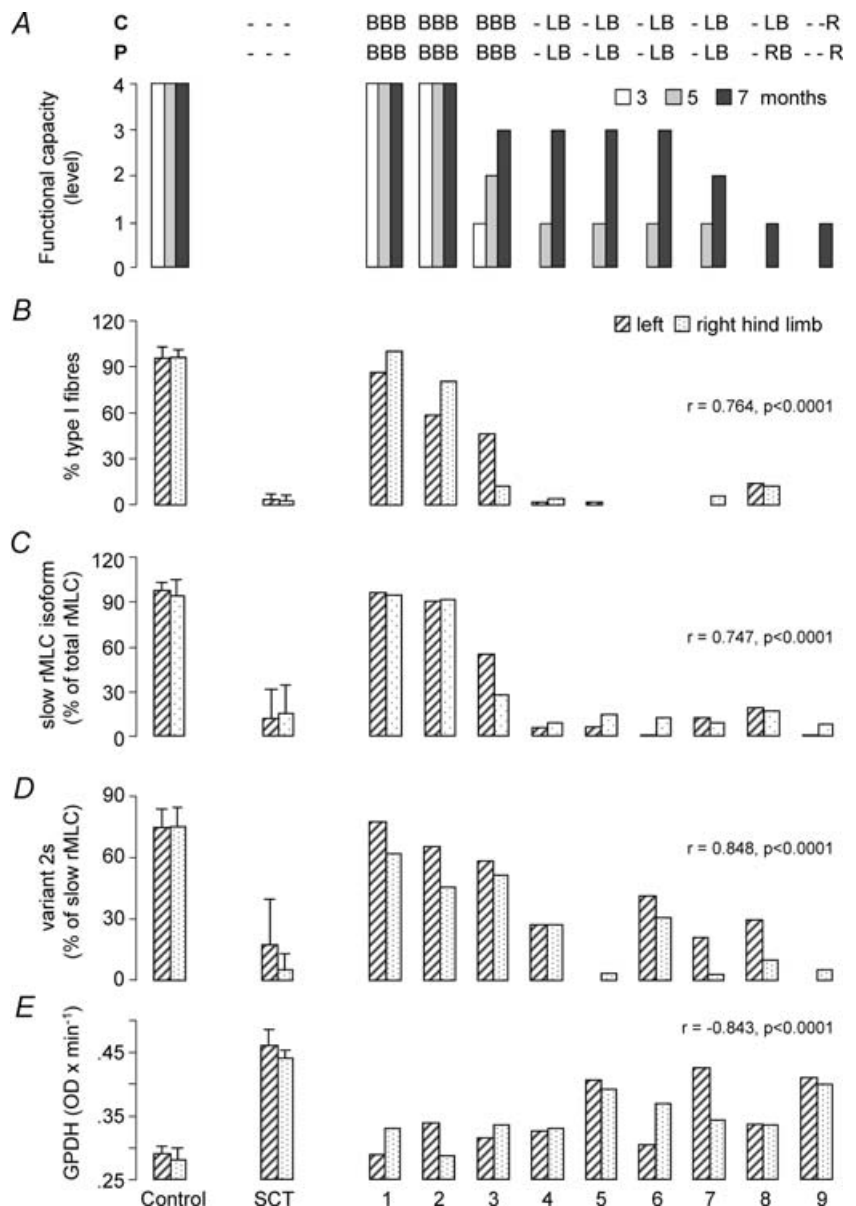
Discussion

The present investigation is to our knowledge the first study to address the impact of OEG transplantation into completely transected spinal cord on the phenotypic characteristics of fast- and slow-twitch hind limb skeletal muscle and to test a variety of phenotypic markers to establish possible correlations between the relative maintenance of normal muscle characteristics and the functional capacity for locomotion derived from behavioural tests.

The main findings of this study are that (a) transplantation of OEG into the transected rat spinal cord results in hind limb skeletal muscle phenotypes that are generally intermediate between paralysed and control and different from both, and that (b) the expression levels of a variety of phenotypic markers of slow- and fast-twitch hind limb skeletal muscle correlate very well with the sensory-motor functional capacity of SCT, OEG-transplanted rats determined by means of behavioural tests. Among all parameters tested, the histochemical glycerol-3-phosphate dehydrogenase activity and the fraction of the less acidic variant (variant 2s) of the slow rMLC isoform, in SOL muscle, were seen as the most sensitive phenotypic marker to estimate the degree that a SOL muscle approaches normal characteristics following SCT and OEG transplantation. Similarly, histochemical GPDH activity and muscle weight (or muscle-somatic index) were the most sensitive markers in EDL muscle. It is noteworthy that this study identified not only components of the contractile machinery as sensitive markers of changes in slow- and fast-twitch skeletal muscle phenotypes in response to SCT and OEG transplantation, but also components of the energy metabolism and muscle mass.

The multivariate analysis performed in this study using diverse markers of skeletal muscle morphology, metabolism and molecular diversity of myosin subunits clearly indicated that fast- and slow-twitch skeletal muscle phenotypes of SCT, OEG-transplanted animals were different from those of non-transplanted and from controls. Taking into account the high percentage of correctly classified observations obtained in this analysis, this result provides solid evidence of the impact of OEG transplantation on maintenance of skeletal muscle properties. In quantitative terms, however, the degree to which fibre type-specific protein expression in hind limb skeletal muscle of OEG-transplanted rats approached normality was highly variable from one animal to the other. It was relatively high only in 3 out of 9 OEG-transplanted animals. The remaining 6 animals, precisely those that showed loss of sensory-motor function 3 months after the intervention, showed muscle phenotypes closer to non-transplanted. Since in normal individuals the expression of fibre type-specific characteristics depends upon proper activation of slow and fast motor neurons (Schiaffino & Reggiani, 1996; Pette & Staron, 2001), a possible interpretation of these data is that in 3 out of 9 animals OEG transplantation enabled re-establishing a functional connectivity of local spinal circuits and descending motor pathways. In a previous study involving the same rats used in this investigation (Ramon-Cueto et al. 2000), long distance regeneration of motor pathways within caudal cord stumps and functional recovery was reported. In this investigation it was not determined whether the regenerated axons established functional connections. In addition, it is not clear how these connections, in the cases that they were formed, could get normal enough to support appropriate activity patterns to reoccur. An additional mechanism for OEG transplants to promote a relative maintenance of skeletal muscle characteristics and apparent functional recovery could rely on compensatory adaptations leading to increased neuromuscular activity and motor automatism. Descending upper motor neuron pathways in the motor cortex exert a main influence on local spinal circuits (central pattern generators) that control the coordinated movements associated with locomotion. Automaticity of movement also depends upon sensory information derived from movement, which becomes the only input to control central pattern generation in SCI individuals. Immediately and for months after SCI, the spinal cord circuitry can adapt and develop functional characteristics eventually enabling it to use some of those spinal pathways that are utilized normally (Edgerton et al. 2006; Wolpaw, 2007), which could underlie the functional recovery observed in these animals.

The rationale for using OEG in regenerative studies of the SC lies in their ability to counteract local inhibitory influences for axon growth, re-establish glial pathways and produce neurotrophic factors which stimulate neuronal gene expression and axonal growth. OEG has been reported to produce nerve growth factor (NGF), neurotrophin (NF) 4/5, neuroregulin, brain-derived neurotrophic factor (BDNF) and NT-3 (Ramon-Cueto & Avila, 1998; Boruch et al. 2001), and to secrete some of them in considerable amounts. In addition, the migratory pattern of OEG suggests that these cells can also respond to external stimuli originating from injured nerve cells and their processes (Boruch et al. 2001). Slow skeletal muscle fibres have also been reported to produce NT-4 in an activity-dependent manner and to promote growth and remodelling of adult motoneuron innervation (Belluardo et al. 2001). Hind limb muscle fibres and lumbar astrocytes have been found to produce HSP70, a stress protein that could also act as a neurotrohic factor critically involved in motoneuron survival (Robinson et al. 2005). Exercise is known to stimulate the regenerative potential of CNS neurons (Doyle & Roberts, 2006), restore neurotrophic factor levels and synaptic plasticity

(Ying *et al.* 2005), and promote a permissive cellular environment for axonal growth (Ghiani *et al.* 2007) following SCI. In carrying out these tasks, exercise mimics and possibly potentiates the effects of OEG transplants on neuronal regeneration and synaptic plasticity. During the first 3 months post-surgery, the rats of this study were allowed to move freely in an open field every day and were trained to climb onto inclined grids at slopes from 45 to 90 deg to make them familiar with the climbing test (Ramon-Cueto *et al.* 2000). Although neurotrophic factor levels were not measured, it is reasonable to assume that for some of them (e.g. BDNF, NF-3, HSP70) and interaction of OEG and exercise could provide the necessary amounts for tropisms to occur, including adaptive changes in central pattern generator. OEG transplants, in concert with exercise, could trigger a sequence of reciprocal cause and effect leading to relative maintenance of skeletal muscle properties that could underlie the functional recovery previously noticed in the rats of this study, in the absence of authentic regeneration of descending cortical pathways. The variety of skeletal muscle phenotypes observed in OEG-transplanted paraplegic rats, as compared with non-transplanted, could arise from adaptive singularities of the spinal circuitry, leading to different levels of activation of motor neurons.

The migratory behaviour and ability to produce neurotrophins of OEGs, in concert with the neurotrophic and synaptogenesic effects of exercise, provide some clues to envisage how neuromuscular activity and muscle use could increase in OEG-transplanted rats. In turn, an increased neuromuscular activity could directly influence the formation and maintenance of synaptic sites (Czeh *et al.* 1978; Landmesser, 1992) and regulate skeletal muscle protein expression (Talmadge, 2000) and mass (Goldspink, 1999; Favier *et al.* 2008).

In this context, the skeletal muscle of OEG-transplanted animals provide an additional opportunity of studying differential gene expression aimed at elucidating the molecular mechanisms leading to relative maintenance of skeletal muscle mass and protein expression patterns. Satellite cell activation and apoptosis, positive (e.g. IGF-1 and MGF) or negative (e.g. IL-6 and myostatin) regulatory muscle growth factors, myogenic regulatory factors (MRFs) and other transcription factors possibly implicated in skeletal muscle remodelling (e.g. calcineurin-sensitive transcription factors NF-AT and MEF2), miRNAs and other translation regulatory factors, proteolysis-modulating molecules and signal transduction protein kinases (e.g. Akt, ERK 1/2) (see Goldspink, 1999; Talmadge, 2000; Baldwin & Haddad, 2001; Spangenburg & Booth, 2003; Koulmann & Bigard, 2006; Frost & Lang, 2007; Favier *et al.* 2008 for a review) are some of the events, molecules and pathways by which OEG transplants in concert with exercise could indirectly affect the skeletal muscle phenotype.

In agreement with previous reports (Talmadge *et al.* 1995, 1999; Roy *et al.* 1999), we observed a severe atrophy of SOL in response to SCT, a dramatic reduction in MHC-I-expressing fibres compensated by an increased number of fibres expressing the fast isoforms IIA and IID/X and a parallel slow-to-fast transition in MLC isoforms (Lee & Braun, 1990), supporting the contractile changes in response to reduced neuromuscular activity (Reiser *et al.* 1985; Sweeney *et al.* 1986; Bottinelli *et al.* 1991, 1994) characteristic of paralysed skeletal muscle. As expected, the slow-to-fast transformation of myosin subunit isoforms was paralleled by an increased activity of glycolysis (Talmadge, 2000; Otis *et al.* 2004). In the EDL muscle (formed by type IIA, IID/X and IIB fibres, in approximately the same proportion), fibre type switching has a narrower range of change during a slow-to-fast transition, implying that EDL would be less sensitive to detect phenotypic changes in response to reduced neuromuscular activity than the SOL. However, contrary to expected, some markers of the EDL proved to be as sensitive in grading the extent that a particular muscle approached normality as SOL markers (i.e. GPDH activity, Fig. 2). Although somehow puzzling, this conclusion is in agreement with observations (Borisov *et al.* 2001) indicating that fast-twitch fibres could be even more susceptible to partial dedifferentiation than slow-twitch fibres and that they possess higher phenotypic plasticity. Since muscle mass and contractility are controlled independently, a combination of morphological and molecular markers of both slow and fast skeletal muscle, as used in this investigation, allowed depiction of a precise figure of the actual skeletal muscle phenotype.

Using the amplitude of the change induced by SCT as a criteria, the degree of maintenance of normal muscle characteristics following OEG transplantation, the coefficient of correlation with behaviourally tested motor functional capacity and the gradation of their expression levels in animals with similar motor functional capacity, we selected the histochemically assessed GPDH activity as a sensitive phenotypic marker for both SOL and EDL muscle (see Fig. 2). The fraction of the less acidic variant (2s) of the slow rMLC isoform (see Fig. 4 and Gonzalez *et al.* 2002), in the SOL, and muscle wet weight (or muscle-somatic index, Fig. 1) in the EDL, were additional sensitive and potentially useful markers to assess muscle phenotype. SDH activity was not useful since in SCT animals a lower proportion of type I and a higher proportion of type IIB fibres (both contributing to lower muscle oxidative capacity) was variously compensated with increased proportions of IIA and IIX/D fibres that tended to increase the oxidative capacity (see Fig. 2).

Practically all parameters assessed in SOL or EDL muscles allowed establishing a good correlation between muscle phenotype and behaviourally tested functional capacity. Individually considered, however, they were

not sensitive enough to accurately assess the degree that a particular skeletal muscle approached normality or to compare muscles from animals with similar functional capacity. The fraction of the less acidic of the variants (variant 2s) of the slow rMLC isoform in the SOL, the muscle-somatic index in the EDL and the histochemical GPDH activity in both muscles, were probably the exceptions. The observation that variant 2s of the slow rMLC was expressed in OEG-transplanted animals at levels statistically non-different from controls supports the notion that it is a sensitive marker of phenotypic changes. This conclusion is in agreement with previous observations made in a model of indirect low-frequency chronic electrical stimulation of fast-twitch muscle (Gonzalez *et al.* 2002) indicating that changes in the proportion of this variant precede any rearrangement of the sarcomere in the fast-to-slow direction.

In conclusion, the results reported in this paper provide evidence that 8 months after a complete mid-thoracic SCT and simultaneous OEG transplantation, the mean phenotypes of fast- and slow-twitch hind limb skeletal muscles are different from those of non-transplanted rats, indicating maintenance of skeletal muscle properties. However, the extent to which muscle phenotypes of OEG-transplanted animals approached normality greatly differed from animal to animal, from substantive in a few cases to marginal in others, correlating with sensory-motor functional capacity previously assessed in the same rats. The histochemical glycerol-3-phosphate dehydrogenase activity in SOL and EDL muscle and the fraction of the less acidic variant (variant 2s) of the slow rMLC isoform in SOL and muscle weight (or muscle-somatic index) in the EDL came into sight as the most sensitive phenotypic marker to estimate the degree that a skeletal muscle approaches normal characteristics following SCT and OEG transplantation. The relatively low proportion of animals that 8 months after OEG transplantation showed patterns of fibre type-specific protein expression close to normality indicated that OEG transplants alone were insufficient to support a consistent and generalized long-term maintenance of normal skeletal muscle characteristics. A productive interaction with exercise is suggested as a possible mechanism underlying OEG-mediated effects on maintenance of skeletal muscle characteristics. Further work is necessary to understand the molecular events probably involved in transducing OEG and exercise-derived signals into skeletal muscle phenotypic changes.

References

Baldwin KM & Haddad F (2001). Effects of different activity and inactivity paradigms on myosin heavy chain gene expression in striated muscle. *J Appl Physiol* **90**, 345–357.

Barnett SC & Riddell JS (2004). Olfactory ensheathing cells (OECs) and the treatment of CNS injury: advantages and possible caveats. *J Anat* **204**, 57–67.

Belluardo N, Westerblad H, Mudo G, Casabona A, Bruton J, Caniglia G, Pastoris O, Grassi F & Ibanez CF (2001). Neuromuscular junction disassembly and muscle fatigue in mice lacking neurotrophin-4. *Mol Cell Neurosci* **18**, 56–67.

Blanco CE, Sieck GC & Edgerton VR (1988). Quantitative histochemical determination of succinic dehydrogenase activity in skeletal muscle fibres. *Histochem J* **20**, 230–243.

Borisov AB, Dedkov EI & Carlson BM (2001). Interrelations of myogenic response, progressive atrophy of muscle fibers, and cell death in denervated skeletal muscle. *Anat Rec* **264**, 203–218.

Boruch AV, Conners JJ, Pipitone M, Deadwyler G, Storer PD, Devries GH & Jones KJ (2001). Neurotrophic and migratory properties of an olfactory ensheathing cell line. *Glia* **33**, 225–229.

Bottinelli R, Betto R, Schiaffino S & Reggiani C (1994). Unloaded shortening velocity and myosin heavy chain and alkali light chain isoform composition in rat skeletal muscle fibres. *J Physiol* **478**, 341–349.

Bottinelli R, Schiaffino S & Reggiani C (1991). Force–velocity relations and myosin heavy chain isoform compositions of skinned fibres from rat skeletal muscle. *J Physiol* **437**, 655–672.

Brooke MH & Kaiser KK (1970). Three 'myosin adenosine triphosphatase' systems: the nature of their pH lability and sulfhydryl dependence. *J Histochem Cytochem* **18**, 670–672.

Czeh G, Gallego R, Kudo N & Kuno M (1978). Evidence for the maintenance of motoneurone properties by muscle activity. *J Physiol* **281**, 239–252.

Delp MD & Duan C (1996). Composition and size of type I, IIA, IID/X, and IIB fibers and citrate synthase activity of rat muscle. *J Appl Physiol* **80**, 261–270.

Doyle LM & Roberts BL (2006). Exercise enhances axonal growth and functional recovery in the regenerating spinal cord. *Neuroscience* **141**, 321–327.

Dupont-Versteegden EE, Houle JD, Gurley CM & Peterson CA (1998). Early changes in muscle fiber size and gene expression in response to spinal cord transection and exercise. *Am J Physiol Cell Physiol* **275**, C1124–C1133.

Edgerton VR, Kim SJ, Ichiyama RM, Gerasimenko YP & Roy RR (2006). Rehabilitative therapies after spinal cord injury. *J Neurotrauma* **23**, 560–570.

Favier FB, Benoit H & Freyssenet D (2008). Cellular and molecular events controlling skeletal muscle mass in response to altered use. *Pflugers Arch* DOI 10.1007/S00424-007-0423-z.

Frost RA & Lang CH (2007). Protein kinase B/Akt: a nexus of growth factor and cytokine signaling in determining muscle mass. *J Appl Physiol* **103**, 378–387.

Ghiani CA, Ying Z, de Vellis J & Gomez-Pinilla F (2007). Exercise decreases myelin-associated glycoprotein expression in the spinal cord and positively modulates neuronal growth. *Glia* **55**, 966–975.

Goldspink G (1999). Changes in muscle mass and phenotype and the expression of autocrine and systemic growth factors by muscle in response to stretch and overload. *J Anat* **194**, 323–334.

Gonzalez B, Negredo P, Hernando R & Manso R (2002). Protein variants of skeletal muscle regulatory myosin light chain isoforms: prevalence in mammals, generation and transitions during muscle remodelling. *Pflugers Arch* **443**, 377–386.

Hartkopp A, Harridge SD, Mizuno M, Ratkevicius A, Quistorff B, Kjaer M & Biering-Sorensen F (2003). Effect of training on contractile and metabolic properties of wrist extensors in spinal cord-injured individuals. *Muscle Nerve* **27**, 72–80.

Hernando R & Manso R (1997). Muscle fibre stress in response to exercise: synthesis, accumulation and isoform transitions of 70-kDa heat-shock proteins. *Eur J Biochem* **243**, 460–467.

Keyvan-Fouladi N, Li Y & Raisman G (2002). How do transplanted olfactory ensheathing cells restore function? *Brain Res Brain Res Rev* **40**, 325–327.

Kjaer M (2000). Why exercise in paraplegia? *Br J Sports Med* **34**, 322–323.

Koulmann N & Bigard AX (2006). Interaction between signalling pathways involved in skeletal muscle responses to endurance exercise. *Pflugers Arch* **452**, 125–139.

Landmesser L (1992). The relationship of intramuscular nerve branching and synaptogenesis to motoneuron survival. *J Neurobiol* **23**, 1131–1139.

Lee JC & Braun AM (1990). Analysis of rat hindlimb muscle proteins by two-dimensional gels following spinal cord injury. *J Neurochem* **54**, 96–101.

Martin TP, Vailas AC, Durivage JB, Edgerton VR & Castleman KR (1985). Quantitative histochemical determination of muscle enzymes: biochemical verification. *J Histochem Cytochem* **33**, 1053–1059.

Nwoye L, Mommaerts WF, Simpson DR, Seraydarian K & Marusich M (1982). Evidence for a direct action of thyroid hormone in specifying muscle properties. *Am J Physiol Regul Integr Comp Physiol* **242**, R401–R408.

Otis JS, Roy RR, Edgerton VR & Talmadge RJ (2004). Adaptations in metabolic capacity of rat soleus after paralysis. *J Appl Physiol* **96**, 584–596.

Pette D & Staron RS (1997). Mammalian skeletal muscle fiber type transitions. *Int Rev Cytol* **170**, 143–223.

Pette D & Staron RS (2001). Transitions of muscle fiber phenotypic profiles. *Histochem Cell Biol* **115**, 359–372.

Prochazka A & Mushahwar VK (2001). Spinal cord function and rehabilitation – an overview. *J Physiol* **533**, 3–4.

Raisman G (2001). Olfactory ensheathing cells – another miracle cure for spinal cord injury? *Nat Rev Neurosci* **2**, 369–375.

Ramon-Cueto A & Avila J (1998). Olfactory ensheathing glia: properties and function. *Brain Res Bull* **46**, 175–187.

Ramon-Cueto A, Cordero MI, Santos-Benito FF & Avila J (2000). Functional recovery of paraplegic rats and motor axon regeneration in their spinal cords by olfactory ensheathing glia. *Neuron* **25**, 425–435.

Ramon-Cueto A & Nieto-Sampedro M (1992). Glial cells from adult rat olfactory bulb: immunocytochemical properties of pure cultures of ensheathing cells. *Neuroscience* **47**, 213–220.

Ramon-Cueto A & Nieto-Sampedro M (1994). Regeneration into the spinal cord of transected dorsal root axons is promoted by ensheathing glia transplants. *Exp Neurol* **127**, 232–244.

Ramon-Cueto A, Perez J & Nieto-Sampedro M (1993). In vitro enfolding of olfactory neurites by p75 NGF receptor positive ensheathing cells from adult rat olfactory bulb. *Eur J Neurosci* **5**, 1172–1180.

Ramon-Cueto A, Plant GW, Avila J & Bunge MB (1998). Long-distance axonal regeneration in the transected adult rat spinal cord is promoted by olfactory ensheathing glia transplants. *J Neurosci* **18**, 3803–3815.

Ramon-Cueto A & Valverde F (1995). Olfactory bulb ensheathing glia: a unique cell type with axonal growth-promoting properties. *Glia* **14**, 163–173.

Reiser PJ, Moss RL, Giulian GG & Greaser ML (1985). Shortening velocity in single fibers from adult rabbit soleus muscles is correlated with myosin heavy chain composition. *J Biol Chem* **260**, 9077–9080.

Rivero JL, Talmadge RJ & Edgerton VR (1999). Interrelationships of myofibrillar ATPase activity and metabolic properties of myosin heavy chain-based fibre types in rat skeletal muscle. *Histochem Cell Biol* **111**, 277–287.

Robinson MB, Tidwell JL, Gould T, Taylor AR, Newbern JM, Graves J, Tytell M & Milligan CE (2005). Extracellular heat shock protein 70: a critical component for motoneuron survival. *J Neurosci* **25**, 9735–9745.

Roy RR, Talmadge RJ, Hodgson JA, Oishi Y, Baldwin KM & Edgerton VR (1999). Differential response of fast hindlimb extensor and flexor muscles to exercise in adult spinalized cats. *Muscle Nerve* **22**, 230–241.

Santos-Benito FF, Munoz-Quiles C & Ramon-Cueto A (2006). Long-term care of paraplegic laboratory mammals. *J Neurotrauma* **23**, 521–536.

Santos-Benito FF & Ramon-Cueto A (2003). Olfactory ensheathing glia transplantation: a therapy to promote repair in the mammalian central nervous system. *Anat Rec* **271B**, 77–85.

Schiaffino S, Gorza L, Sartore S, Saggin L, Ausoni S, Vianello M, Gundersen K & Lomo T (1989). Three myosin heavy chain isoforms in type 2 skeletal muscle fibres. *J Muscle Res Cell Motil* **10**, 197–205.

Schiaffino S & Reggiani C (1996). Molecular diversity of myofibrillar proteins: gene regulation and functional significance. *Physiol Rev* **76**, 371–423.

Shields RK & Dudley-Javoroski S (2006). Musculoskeletal plasticity after acute spinal cord injury: effects of long-term neuromuscular electrical stimulation training. *J Neurophysiol* **95**, 2380–2390.

Snow DH & Guy PS (1980). Muscle fibre type composition of a number of limb muscles in different types of horse. *Res Vet Sci* **28**, 137–144.

Spangenburg EE & Booth FW (2003). Molecular regulation of individual skeletal muscle fibre types. *Acta Physiol Scand* **178**, 413–424.

Staron RS & Pette D (1993). The continuum of pure and hybrid myosin heavy chain-based fibre types in rat skeletal muscle. *Histochemistry* **100**, 149–153.

Sweeney HL, Kushmerick MJ, Mabuchi K, Gergely J & Sreter FA (1986). Velocity of shortening and myosin isozymes in two types of rabbit fast-twitch muscle fibers. *Am J Physiol Cell Physiol* **251**, C431–C434.

Talmadge RJ (2000). Myosin heavy chain isoform expression following reduced neuromuscular activity: potential regulatory mechanisms. *Muscle Nerve* **23**, 661–679.

Talmadge RJ, Roy RR & Edgerton VR (1995). Prominence of myosin heavy chain hybrid fibers in soleus muscle of spinal cord-transected rats. *J Appl Physiol* **78**, 1256–1265.

Talmadge RJ, Roy RR & Edgerton VR (1999). Persistence of hybrid fibers in rat soleus after spinal cord transection. *Anat Rec* **255**, 188–201.

Wernig A, Nanassy A & Muller S (1999). Laufband (treadmill) therapy in incomplete paraplegia and tetraplegia. *J Neurotrauma* **16**, 719–726.

Wewetzer K, Verdu E, Angelov DN & Navarro X (2002). Olfactory ensheathing glia and Schwann cells: two of a kind? *Cell Tissue Res* **309**, 337–345.

Wolpaw JR (2007). Spinal cord plasticity in acquisition and maintenance of motor skills. *Acta Physiol (Oxf)* **189**, 155–169.

Ying Z, Roy RR, Edgerton VR & Gomez-Pinilla F (2005). Exercise restores levels of neurotrophins and synaptic plasticity following spinal cord injury. *Exp Neurol* **193**, 411–419.

Acknowledgements

Author's present address

P Negredo: Department of Clinical Pharmacology, Faculty of Medicine, Autonomous University of Madrid, E-28029 Madrid, Spain. B González: The Scripps Research Institute, La Jolla, CA, USA.